Identifying Inhibitors of Epithelial-Mesenchymal Transition by Connectivity Map–Based Systems Approach

Ajaya Kumar Reka, PhD, Rork Kuick, MS,† Himabindu Kurapati, MSc,* Theodore J. Standiford, MD,* Gilbert S. Omenn, MD, PhD,‡ and Venkateshwar G. Keshamouni, PhD**

Background: Acquisition of mesenchymal phenotype by epithelial cells by means of epithelial-mesenchymal transition (EMT) is considered as an early event in the multistep process of tumor metastasis. Therefore, inhibition of EMT might be a rational strategy to prevent metastasis.

Methods: Using the global gene expression profile from a cell culture model of transforming growth factor-β (TGF-β)-induced EMT, we identified potential EMT inhibitors. We used a publicly available database (www.broad.mit.edu/cmap) comprising gene expression profiles obtained from multiple different cell lines in response to various drugs to derive negative correlations to EMT gene expression profile using Connectivity Map, a pattern matching tool.

Results: Experimental validation of the identified compounds showed rapamycin as a novel inhibitor of TGF-β signaling along with 17-AAG, a known modulator of TGF-β pathway. Both of these compounds completely blocked EMT and the associated migratory and invasive phenotype. The other identified compound, LY294002, demonstrated a selective inhibition of mesenchymal markers, cell migration and invasion, without affecting the loss of E-cadherin expression or Smad phosphorylation.

Conclusions: Our data reveal that rapamycin is a novel modulator of TGF-β signaling, and along with 17-AAG and LY294002, could be used as therapeutic agent for inhibiting EMT. This study demonstrates the potential of a systems approach in identifying novel modulators of a complex biological process.

Key Words: TGF-beta, Epithelial-mesenchymal transition, Connectivity map, Lung cancer, mTOR, PI3K, HSP90.

(*J Thorac Oncol.* 2011;6: 1784–1792)

*Division of Pulmonary and Critical Care Medicine, Department of Internal Medicine; †Comprehensive Cancer Center, University of Michigan Medical Center; and ‡Departments of Internal Medicine and Human Genetics, Medical School, School of Public Health and Center for Computational Medicine and Bioinformatics and Michigan Proteomics Alliance for Cancer Research, University of Michigan, Ann Arbor, Michigan.

Disclosure: The authors declare no conflicts of interest.

Address for correspondence: Venkateshwar G. Keshamouni, PhD, Division of Pulmonary and Critical Care Medicine, Department of Internal Medicine, University of Michigan Medical Center, 4062 BSRB, 109 Zina Pitcher Place, Ann Arbor, MI 48109. E-mail: vkeshamo@med.umich.edu

ISSN: 1556-0864/11/0611-1784

Metastasis is the major cause of mortality in cancer-related deaths. Hence, determining and targeting precise molecular mechanisms of metastasis is critical for a successful prevention strategy. During metastasis, cancer cells acquire the ability to invade surrounding tissue with subsequent dissemination to secondary organs.[1] The acquisition of migratory and invasive capability by otherwise stationary epithelial cells is associated with gain of mesenchymal characteristics and concomitant loss of epithelial phenotype, a phenomenon referred to as epithelial-mesenchymal transition (EMT).[2] EMT also confers resistance to anoikis, evasion of immune surveillance, and in certain cases is associated with stem cell-like properties of the resulting mesenchymal cells, all of which may be required for a cancer cell to successfully metastasize. Therefore, inhibition of EMT might be a rational strategy to prevent metastasis.

The cytokine transforming growth factor-β (TGF-β) plays a paradoxical role in cancer biology, whereby it acts as a tumor suppressor in early stages and as a tumor promoter in late stages of tumor progression. The tumor-promoting functions of TGF-β include induction of EMT in cancer cells.[3–5] Depending on the cell type and context, TGF-β induces EMT by activation of multiple signaling pathways, both Smad-dependent and Smad-independent, and cross talk with developmental pathways like WNT and Notch signaling.[6–9] Given the complex nature of EMT regulation, it is challenging to identify critical regulatory molecules or pathways for targeting EMT.

System-wide profiling of molecular changes offers an opportunity to understand the underlying mechanisms and design strategies to perturb the system.[10] Gene expression profiling represents all the transcriptional alterations happening in a given disease state and time. Compounds that can reverse some, if not all, of these changes might serve as potential inhibitors of that particular disease state. A recently developed pattern matching tool known as Connectivity Map (C-Map) has demonstrated its utility in identifying potential inhibitors using gene expression profiles of a given biological state. The C-Map tool is built on a database comprised of 564 gene expression profiles derived from multiple cell lines after treatment with 164 different compounds at different doses (453 profiles or "instances"), along with 111 corresponding controls.[11] Using C-Map, one can derive negative correlations between the gene expression perturbations of the biological state of interest and the perturbations of each drug

instance in the database. The drugs whose instances are most significantly correlated are ones that may serve as potential inhibitors of that particular state; in this case it is EMT. Using C-Map, we analyzed the global gene expression profile obtained from TGF-β-induced EMT in the A549 lung adenocarcinoma cell line to identify potential inhibitors of EMT. We identified known and new potential EMT inhibitors. Validation of these compounds for EMT inhibition revealed their novel mechanism of action and the potential of targeting mammalian target of rapamycin (mTOR), HSP90, and PI3K pathways for inhibiting EMT, tumor cell migration and invasion.

EXPERIMENTAL PROCEDURES

EMT Experiment with Test Compounds

A549 (human lung adenocarcinoma) and H358 (human bronchioalveolar carcinoma) cell lines were obtained from the American Type Culture Collection (Manassas, VA) and maintained in Roswell Park Memorial Institute 1640 medium with supplemented with 10% fetal bovine serum, glutamine, penicillin, and streptomycin at 37°C in 5% CO_2. The authentication of cell lines was not performed by authors. In all experiments, cells at 40% to 50% confluency in complete medium were serum starved for 24 hours and were treated with TGF-β (5 ng/ml) for 72 hours in the presence and absence of compounds at indicated concentrations. Test compounds were added to the cultures 30 minutes before TGF-β stimulation. After 72 hours, cells were either lysed for assessing protein expression or trypsinized for replating in the transwell chambers for assessing migration and invasion. The conditioned media was collected for estimation of matrix metallo proteases (MMPs). All the test compounds used in this study were purchased from Tocris Biosciences, USA.

Gene Expression and C-Map Analysis

A549 lung-cancer cells were treated with 5 ng/ml of TGF-β and harvested at various time points in three separate experiments, and the resulting RNA collected, assayed using Affymetrix HG-U133_plus_2 arrays, and analyzed as previously described.[12] We used probe set annotation from Affymetrix web sites (version na30, dated November 13, 2009). Using two-way analysis of variance models with terms for the three experiments and nine time points, we selected probe sets that gave p less than 0.001 for each time point compared with the 0 hour control samples and also gave average fold-differences of at least 1.5-fold. This data set and the p values and fold-differences obtained are publicly available as GEO series GSE17708.[12] We formed the union of the selected probe sets for the 0.5-, 1-, and 2-hour time points as a representative list of early-responding genes, and the union of 4 and 8 hours as representative list of intermediate-responding genes. For the three early time points, this yielded 478 probe sets increased with TGF-β and 244 decreased, of which 237 and 113, respectively, were also on the smaller Affymetrix U133A (or similar HT_HG-U133A) arrays, which are the arrays used to generate data on the effects of various compounds by Lamb et al.[13] in their work on "The Connectivity Map." For the union of 4 and 8 hours time points, we obtained 1884 increased and 1254 decreased probe sets, of which 1006 and 703 were on U133A arrays. The C-Map data consist of 164 compounds tested on several cell lines (MCF7, PC-3, HL-60, and SKMEL5), with a total of 453 treatments, called instances, and 111 arrays of appropriate control treatments (564 total arrays). We input our list of up and down probe sets, given values of 1 and -1, into the software of Zhang and Gant,[14] which computes Cscores that are similar to correlation coefficients between our values and the ranks of the ratios of treatment to the average of controls for the instances of Lamb et al. Negative Cscores indicate the compound altered probe sets in an opposite-correlated way compared with the differences we observed with TGF-β treatment. The software computes similar scores in 10,000 additional runs in which the probe set labels are randomly permuted and computes two-sided permutation test p values as the fraction of scores from permuted data sets with larger absolute value than the one actually obtained for the instance. To judge the significance of compounds, Cscores for the instances of the compound are averaged to compute the SetCscore for each compound, and this averaging is also performed on the permuted data sets, and the software again computes permutation test p values. With only 10,000 permuted data sets, these p values can be no smaller than 0.0001; however, the means and standard deviations of the SetCscores from permutations are also reported, enabling us to obtain a finer-grained test of significance by dividing the SetCscore by this standard deviation and computing two-sided tests by referring this standardized SetCscore to standard Normal (Gaussian) distributions. For p values of approximately 0.0001 and larger the two methods agreed fairly well, but for the largest SetCscores the p values from standardized SetCscores were much smaller, as expected, and enabled us to better judge the relative evidence in favor of the top-scoring compounds.

Fluorescence Microscopy

Cells treated in 48-well tissue culture plates were fixed in 4% formalin, blocked with 5% horse serum, permeabilized with 0.3% Triton-X 100 and stained with FITC conjugated E-cadherin antibody overnight at 4°C. Subsequently, cells were washed with phosphate-buffered saline and stained sequentially for F-actin with Rhodamine Phalloidin and for nuclei with DAPI. Images were captured using a fluorescent microscope (EVOS*fl,* Bothell, WA) at 20× magnification. Images were processed by Adobe Photoshop (Adobe Systems Inc., San Jose, CA).

Cell Migration and Invasion Assays

In vitro migration assays were performed as previously described.[15] Briefly, cells were seeded in the top chamber of the 8.0 μm pore size cell culture inserts that were either coated or uncoated with matrigel for migration and invasion assays, respectively. Then the inserts were placed in a 24-well plate filled with Roswell Park Memorial Institute 1640 medium with 5% fetal bovine serum. Cells that penetrated to the underside surfaces of the inserts were fixed and stained with the Diff-Quick (Fisher Scientific, Pittsburgh, PA) method and were counted under the microscope. The mean of three

high power fields for each condition run in triplicates was calculated.

Western Blot

Samples containing 20 μg of total protein were electrophoresed on SDS–polyacrylamide gels and transferred onto a polyvinyldifluoride membrane by electroblotting. Membranes were probed with primary antibodies with overnight incubation at 4°C, followed by horseradish peroxidase–conjugated secondary antibodies. Finally, the immunoblots were visualized by using ECL reagents.

Smad Transcriptional Activity

Effect of test compounds on Smad transcriptional activity was determined in A549-SBE (Smad Binding Elements)-Luc cells as previously described.[15] Briefly, cells were serum starved overnight and treated with TGF-β (5 ng/ml) in presence and absence of compounds pretreatment. After 4 hours, luciferase activity was measured using the steady-glo luciferase kit (from Promega, USA) as per the manufacturer's instructions. Luciferase counts were normalized to the total protein concentrations in the respective samples.

Statistical Analysis

Data are represented as mean ± standard deviations and were analyzed with the Prism version 4.0 statistical program (GraphPad Software, San Diego, CA). Groups were compared using one-way analysis of variance or student *t* test. Differences were considered significant if p less than 0.05.

RESULTS

C-Map Analysis using Early Gene Expression Changes during EMT-Identified Potential Inhibitors of EMT

Stimulation of cells with TGF-β induces activation and nuclear translocation of transcription factors Smad2 and Smad3.[16] This results in the subsequent robust transcriptional regulation of the target genes. These transcriptional changes are critical for the regulation of TGF-β-induced complex biological responses including EMT.[16] Reversal of these transcriptional changes may be critical for inhibiting EMT. Therefore, to identify inhibitors of EMT, we derived a list of TGF-β-responding (increased and decrease) probe sets in EMT, from the union of three time points (0.5, 1, and 2 hours) from a time course gene expression analysis of TGF-β-induced EMT in the A549 lung adenocarcinoma cell line.[12] Using the C-Map tool, we computed connectivity scores (Cscores) between this EMT profile and the 453 instances in Lamb et al.[13] data base from 164 compounds. Cscores are similar to correlation coefficients, and a negative Cscore indicates that the compound from which that instance is derived potentially reverses the gene expression changes in the input profile, which in this case was EMT. The Cscores for the instances were averaged to obtain SetCscores for each compound, and we standardized these by dividing the standard deviation of the SetCscores for the same compound, obtained from 10,000 data sets in which the probe set labels were randomly permuted. We identified 49 negatively correlated compounds with p less than 0.01, of which 30 gave p less than 0.0001. To focus on the most reliable findings, we reduced these 30 candidates to 21 compounds that had at least two instances, which are shown in Table 1. Because a total of 95 compounds had at least two instances, we expect only approximately 0.01 ($=0.0001\times95$) false-positive compounds using this selection criterion. Compounds identified include inhibitors of HSP90, PI3K, mTOR, cycloxygenase, prostaglandin synthetase, DNA gyrase, Rho-Kinase, Calcineurin, purine synthesis, α-estradiol, and aromatase. Interestingly, for all 21 compounds, either the compounds themselves or the primary pathways that the compounds are known to inhibit were implicated in cancer (Table 1). This includes the unanticipated, antipsychotic compounds Chlorpromazine and Clozapine, which have also shown to inhibit cancer cell growth.[27,39] Complete analysis and the Cscores derived for all the instances are presented in Supplementary Table 1 (http://links.lww.com/JTO/A128). Similar analysis with the gene profile derived from the union of 4- and 8-hour time points also largely identified the same compounds (Supplementary Table 1, http://links.lww.com/JTO/A128) with compound scores for two temporal profiles being highly correlated ($r = 0.90$ for 95 compounds, $p = 1 \times 10^{-34}$).

Experimental Validation of Compounds Identified by the C-Map Analysis

EMT is characterized by loss of epithelial markers (E-cadherin) and gain of mesenchymal markers (N-cadherin, Vimentin) resulting in the acquisition of migratory and invasive phenotype. Hence, to test the ability of the compounds identified by C-Map analysis, to inhibit EMT, we assessed their effects on biochemical markers and functional attributes of EMT in two different cell culture models, A549 and H358. A549 Cells were stimulated with TGF-β (5 ng/ml) in the presence and absence of test compounds at indicated concentrations and assessed stress-fiber formation, expression of epithelial and mesenchymal markers by immunofluorescence microscopy and western immunoblotting (Figures 1*A*, *B*). Consistent with EMT, 72 hours TGF-β treatment significantly suppressed the E-cadherin expression compared with the untreated controls (Figures 1*A*, *B*). However, the presence of rapamycin (Sirolimus, mTOR inhibitor) or 17-AAG (HSP90 inhibitor) completely reversed TGF-β-induced suppression of E-cadherin expression, at all concentrations tested (Figures 1*A, B*). Further, both the compounds also blocked basal and TGF-β-induced up-regulation of mesenchymal marker N-cadherin. Treatment of Rapamycin and 17-AAG alone induced a slight increase in the basal vimentin levels in the control cells, but it was not statistically significant (Supplementary Figure 1, http://links.lww.com/JTO/A129). Although rapamycin had no effect, 17-AAG completely abrogated the TGF-β-induced vimentin expression (Figure 1*B*). Interestingly, LY294002 had no effect on TGF-β-induced E-cadherin suppression (Figures 1*A*, *B*), but attenuated both the basal and TGF-β-induced up-regulation of N-cadherin and vimentin, suggesting a selective effect on mesenchymal phenotype (Figure 1*B*). Consistent with their effect on mes-

TABLE 1. Top Scoring Compounds in C-Map Analysis: The 21 Compounds with Probe Set alterations Negatively Correlated to Early (0.5, 1, and 2 h) Alterations Observed with TGF-β Treatment are Given

Compound	Set Size	Standardized SetCscore (0.5, 1, 2 h)	*p* Value from Standardized SetCscore (*Z*-Score)	Mode of Action	Relevance in Cancer (Reference)
17-Allylamino-geldanamycin	18	−7.73	1.07E − 14	HSP90 inhibitor	17, 18
LY294002	17	−5.91	3.41E − 09	PI3K inhibitor	19, 20
Sirolimus (Rapamycin)	10	−4.72	2.36E − 06	mTOR inhibitor	19, 21
Geldanamycin	6	−5.33	1.01E − 07	HSP90 inhibitor	17, 18
Novobiocin	6	−4.17	3.10E − 05	DNA Gyrase inhibitor	22, 23
Nordihydroguaiaretic acid	5	−5.20	1.96E − 07	Cyclooxygenase inhibitor	24, 25
Staurosporine	4	−5.42	5.87E − 08	Protein Kinase C inhibitor	26
Chlorpromazine	4	−4.84	1.31E − 06	Dopamine and seretonin receptor antagonist	27
SC-58125	4	−4.01	5.96E − 05	Cyclooxygenase inhibitor	28
LM-1685	3	−5.50	3.81E − 08	Cyclooxygenease inhibitor	25, 29
Acetylsalicylic acid	3	−5.36	8.46E − 08	Cyclooxygenase inhibitor	25, 30
17-dimethylamino-geldanamycin	2	−6.39	1.67E − 10	HSP90 inhibitor	17, 18
Cyclosporin	2	−5.41	6.40E − 08	Calcineurin inhibitor	31, 32
Fasudil	2	−5.23	1.71E − 07	Rho-kinase inhibitor	33
Mercaptopurine	2	−5.17	2.40E − 07	Purine synthesis inhibitor	34
Oxaprozin	2	−5.16	2.52E − 07	Prostaglandin synthetase inhibitor	35
Diclofenac	2	−4.85	1.26E − 06	Cyclooxygenase inhibitor	25
4,5-Dianilinophthalimide	2	−4.68	2.88E − 06	Multikinase inhibitor	36
NU-1025	2	−4.62	3.77E − 06	PARP inhibitor	37
Butein	2	−4.41	1.03E − 05	Aromatase inhibitor	38
Clozapine	2	−3.91	9.05E − 05	Dopamine and serotonin receptor antagonist	39

Each compound was represented by at least two instances (SetSize) and gave $p < 0.0001$ for a *Z*-score test of the average Cscores for all the instances of the compound (SetCscores). The *p* values are two-sided tests based on the standardized SetCscore, which were the SetCscores divided by the standard deviation of this score computed from 10,000 random permutations of the probe set labels. Detailed results for all 164 compounds are given in Supplementary Table.

C-map, Connectivity Map; mTOR, mammalian target of rapamycin.

enchymal phenotype, all the three compounds inhibited TGF-β-induced change in morphology and stress fiber formation in A549 cells (Figure 1*A*). Reflecting their effect on epithelial and mesenchymal markers, rapamycin and 17-AAG inhibited EMT-induced cellular migration and invasion in A549 cells (Figure 2). These two compounds also blocked concomitant secretion of MMP2 and MMP9 during EMT (Data not shown). Interestingly, LY294002, which only inhibited mesenchymal markers, also inhibited EMT-induced cellular migration, invasion (Figure 2*A*) and MMP secretion (Data not shown). All the above three compounds, demonstrated similar effects on expression of E-cadherin and vimentin (Figure 1*C*), and cellular invasion (Figure 2) during TGF-β-induced EMT in H358 cells, another non-small cell lung cancer cell line. This demonstrates that the observed effects of these compounds are not specific to a single cell line (Supplementary Figure 1 and Supplementary Table 2, http://links.lww.com/JTO/A128).

From the list of compounds identified, we also assessed the effect of acetylsalicyclic acid and novobiocin on TGF-β-induced EMT. At the concentrations tested, both these compounds showed no significant effects on either biochemical or functional markers (migration and invasion) of EMT (data not shown). However, we have not ruled out the effect of these two compounds on the other functional phenotypes conferred by EMT, including growth inhibition, resistance to apoptosis, evasion of immune surveillance and, in certain cases, stem cell-like properties.[2,40]

Effect of Rapamycin, 17-AAG, and LY294002 on Smad Phosphorylation and Transcriptional Activation

TGF-β induces robust phosphorylation of Smad 2 and 3, by TGF-β-receptor-I kinase, within 1 hour and persists beyond 4 hours. Both Smad-dependent and independent signaling pathways were implicated in TGF-β-induced EMT.[8] However, in different cells, we and others[41] have shown that activation of Smad3 is indispensible for TGF-β-induced EMT, including in A549 cells.[42] We tested the above three compounds for their potential effects on TGF-β-induced Smad phosphorylation. A549 cells were stimulated with TGF-β for 1 hour in the presence and absence of LY-294002 or rapamycin or 17-AAG at indicated concentrations and assessed for Smad2 and Smad3 phosphorylation by western immuno-blotting. All three compounds had no effect on Smad2 or Smad3 phosphorylation after 1 hour of TGF-β

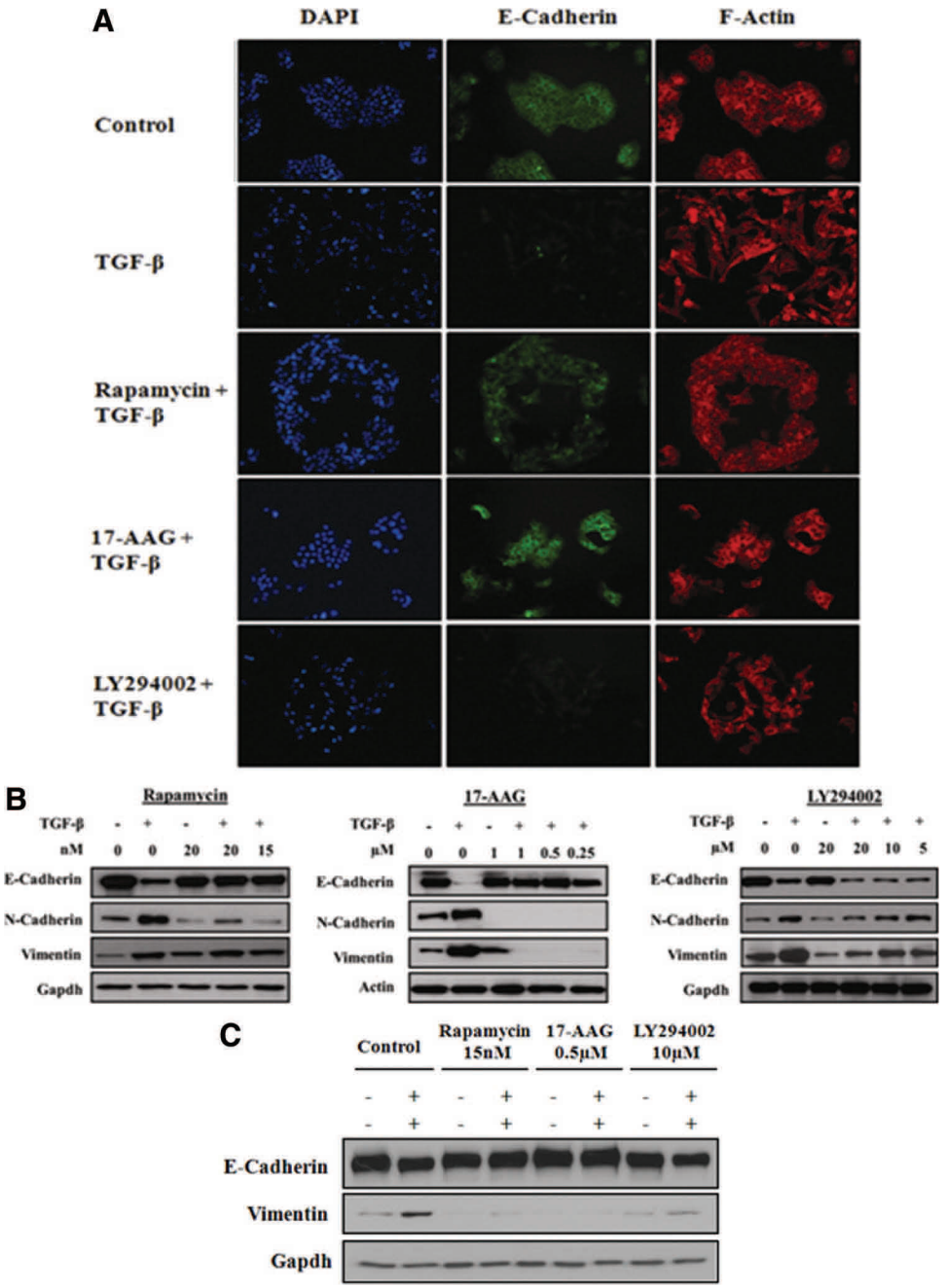

FIGURE 1. Effect of rapamycin, 17-AAG and LY 294002 on Epithelial and mesenchymal markers during transforming growth factor-β (TGF-β) induced epithelial-mesenchymal transition (EMT). A549 or H358 cells were serum starved for 24 hours, pretreated with inhibitors and stimulated with or without TGF-β (5 ng/ml). After 72 hours, (*A*) E-cadherin and stress fibers (F-actin by Phalloidin staining) were assessed in A549 cells by immunofluorescence (scale bar 100 μm), (*B*) epithelial (E-cadherin) and mesenchymal (N-cadherin, vimentin) markers were assessed in A549 cells, (*C*) epithelial (E-cadherin) and mesenchymal (vimentin) markers in H358 cells were assessed by western immunoblotting. Quantitation of western immunoblotting data from three independent experiments was done by ImageJ software and presented in Supplementary Figure S1.

stimulation (Figure 3*A*). This demonstrates that none of these three compounds have any nonspecific effect on the TGF-β-receptor-I kinase.

In a recent study, HSP90 was shown to be critical for the stability of TGF-β receptors, after stimulation with TGF-β, for a sustained Smad phosphorylation. As a result, inhibitors of HSP90 had no effect on immediate Smad phosphorylation within an hour, but blocked sustained Smad phosphorylation as they triggered slow degradation of TGF-β-receptors.[43] Consistent with these findings we observed a

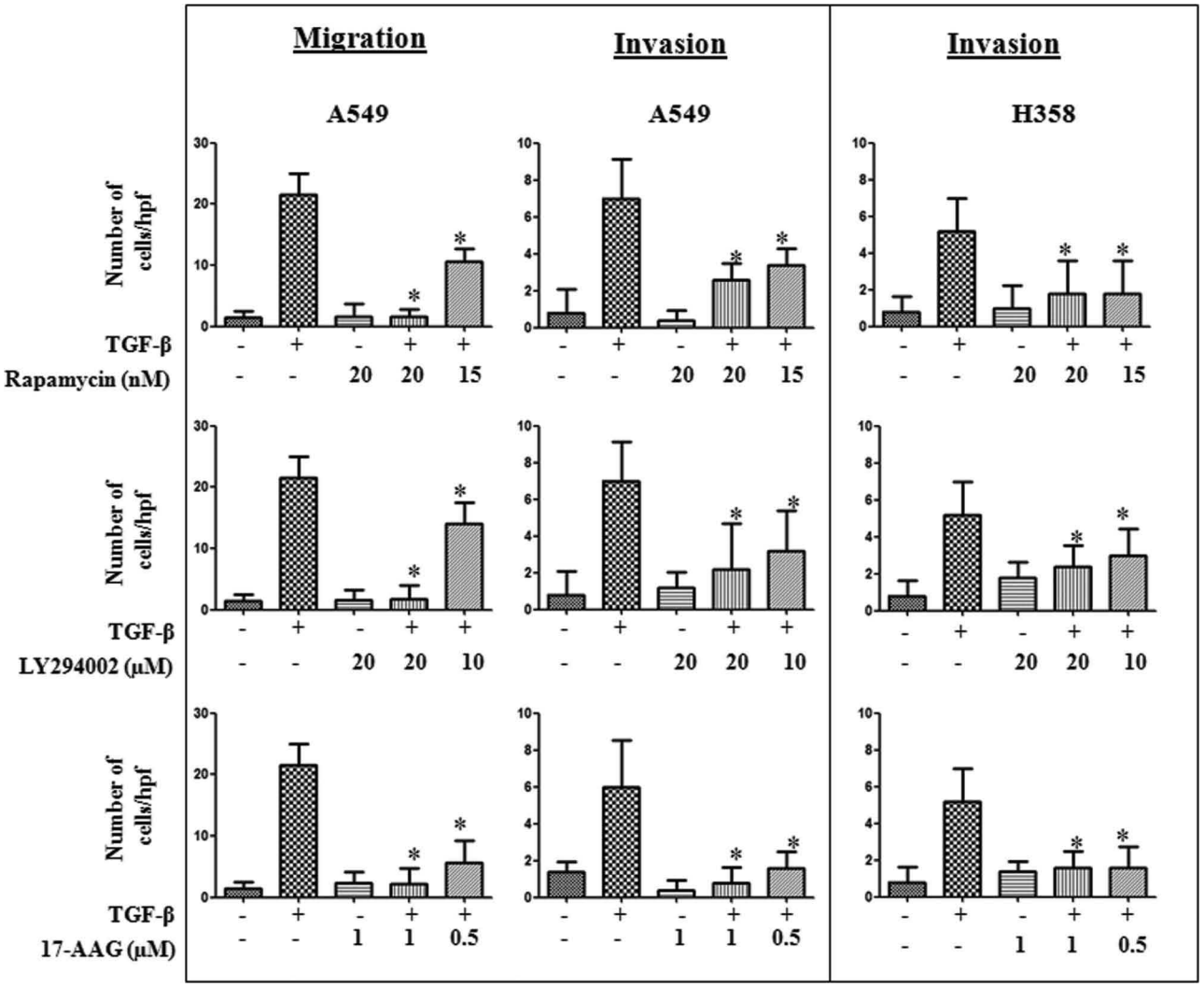

FIGURE 2. Effect of rapamycin, 17-AAG and LY 294002 on migration and invasion during transforming growth factor-β (TGF-β) induced epithelial-mesenchymal transition (EMT): A549 or H358 cells were serum starved for 24 hours, stimulated with TGF-β (5 ng/ml) in the presence or absence of inhibitors at indicated concentrations. After 72 hours, cells were trypsinized and plated in uncoated or matrigel-coated transwell chambers to assess cellular migration and invasion, respectively. Error bars represent the standard deviation (SD) from three independent replicates. *Statistically significant ($p < 0.05$) difference when compared with TGF-β treated cells.

total inhibition of Smad phosphorylation after 4 hours of TGF-β stimulation (Figure 3*B*). Interestingly, in contrast to its effect at 1 hour time point, rapamycin also blocked Smad phosphorylation at 4 hours after TGF-β stimulation (Figure 3*B*), whereas LY294002 had no effect on Smad phosphorylation at either time points (Figures 3*A*, *B*).

Effect of Rapamycin, 17-AAG, and LY294002 on Smad Transcriptional Activity

Following TGF-β stimulation, phosphorylated Smad 2 or 3 translocate into the nucleus as Smad 2/4 or Smad 3/4 heterodimers, bind to the SBE in the promoters of their target genes and trigger gene transcription. To determine whether these compounds had any effect on TGF-β-induced Smad transcriptional activity, we tested the effect of these compounds in the presence and absence of TGF-β in A549 cells stably transfected with a Lentiviral based SBE-Luciferase reporter plasmid. Consistent with the inhibition of Smad phosphorylation, both 17-AAG and rapamycin significantly inhibited the TGF-β induced Smad transcriptional activity (Figures 4*A*, *B*). Surprisingly, although LY294002 had no effect on smad phosphorylation, it inhibited the TGF-β-induced transcriptional activation (Figure 4*C*).

DISCUSSION

Recently, several groups successfully identified and validated potential modulators of different biological processes by analyzing the gene expression profiles using C-Map approach.[11,44–46] C-Map analysis does not require previous

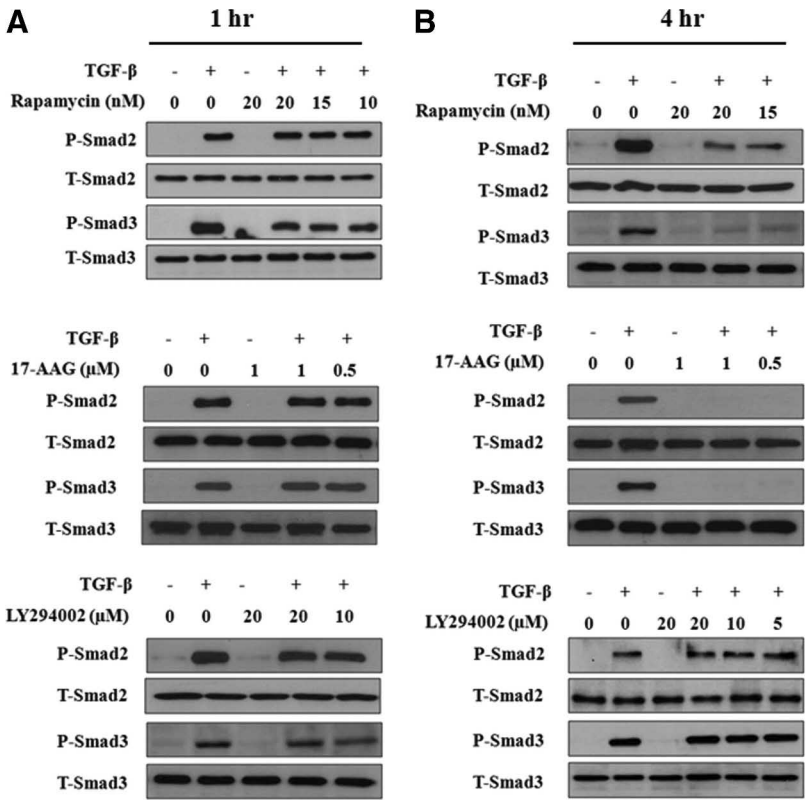

FIGURE 3. Effect of rapamycin, 17-AAG and LY 294002 on transforming growth factor-β (TGF-β) induced Smad phosphorylation: A549 cells were serum starved for 24 hours, stimulated with TGF-β (5 ng/ml) in the presence or absence of inhibitors for 1 (A) or 4 (B) hours. Cell lysates were assessed for phospho-Smad 2 and 3 and total Smad 2 and 3 protein levels by western immunoblotting.

knowledge of the molecules or pathways involved in a biological process. Instead, by simply using the pattern of gene expression alterations under study, compounds that can potentially reverse those alterations and therefore can serve as potential inhibitors of the process can be identified. Using this approach, we identified 21 compounds with various mechanisms of action as potential inhibitors of EMT and validated their affects in two independent TGF-β induced EMT models.

Experimental validation of hits from C-Map analysis identified rapamycin as a novel inhibitor of TGF-β signaling and a potent inhibitor of EMT. Rapamycin in complex with FKBP12 interacts with mTOR and inhibits its activity in the mTOR C1 complex.[47] mTOR activity is increased in many tumors, including lung cancer[48]; inhibition of mTOR function through rapamycin analogues is considered as promising therapeutic strategy. Earlier reports have suggested that activation of mTOR is a Smad-independent TGF-β pathway that regulates protein synthesis, complementing the Smad-mediated transcriptional regulation.[49] Studies with NMuMG mouse mammary epithelial cells and HaCat human keratinocytes showed no effect of rapamycin on TGF-β-induced EMT; however, rapamycin blocked EMT-associated increase in cell size and invasion in these cells.[49] In contrast, we observed a potent inhibition of TGF-β-induced EMT by rapamycin in both A549 and H358 models of EMT. The effect of rapamycin on EMT was evident at the level of both biochemical markers (preventing the loss of E-cadherin and gain of N-cadherin proteins) and at the resulting functional phenotype (inhibition of migration and invasion). This discrepancy might be indicative of a potential difference in TGF-β signaling between malignant (A549) and nonmalignant (NMuMG and HaCat) cells.

The most surprising observation was the effect of rapamycin on TGF-β-induced Smad phosphorylation. Rapamycin significantly inhibited phosphorylation of Smad2 and Smad3 at 4 hours, but not at 1 hour, after TGF-β stimulation. This clearly indicates that the effect of rapamycin on Smad phosphorylation is not due to a nonspecific or off-target effect on TGF-β receptor-I kinase. The HSP90 inhibitor 17-AAG demonstrated similar kinetics in inhibiting Smad phosphorylation (Figures 3*A*, *B*). This is consistent with the recent finding that HSP90 is critical for the stability of TGF-β receptors and required longer duration of drug treatment to observe significant degradation of TGF-β receptors.[43] Accordingly, 17-AAG was also a potent inhibitor of EMT in this study in both cell types tested. Given the similarity between the effects of rapamycin and 17-AAG, it may be important to investigate the role of rapamycin and potentially mTOR in regulating the stability of TGF-β receptors, particularly in cancer cells. As opposed to our observations, earlier studies have reported potentiation of TGF-β signaling with rapamycin.[50] FKBP12, the protein to which rapamycin binds, interacts with TGFβRI to inhibit activation of Smads.[50,51] It was suggested that presence of rapamycin sequesters FKBP12 from TGFβRI to potentiate TGF-β signaling.[52] These observations were primarily made in nonmalignant epithelial cells and predominantly from the NMuMG mouse mammary epithelial cell line. It would be interesting to investigate whether the FKBP12 pathway is still functional in cancer cells and, if

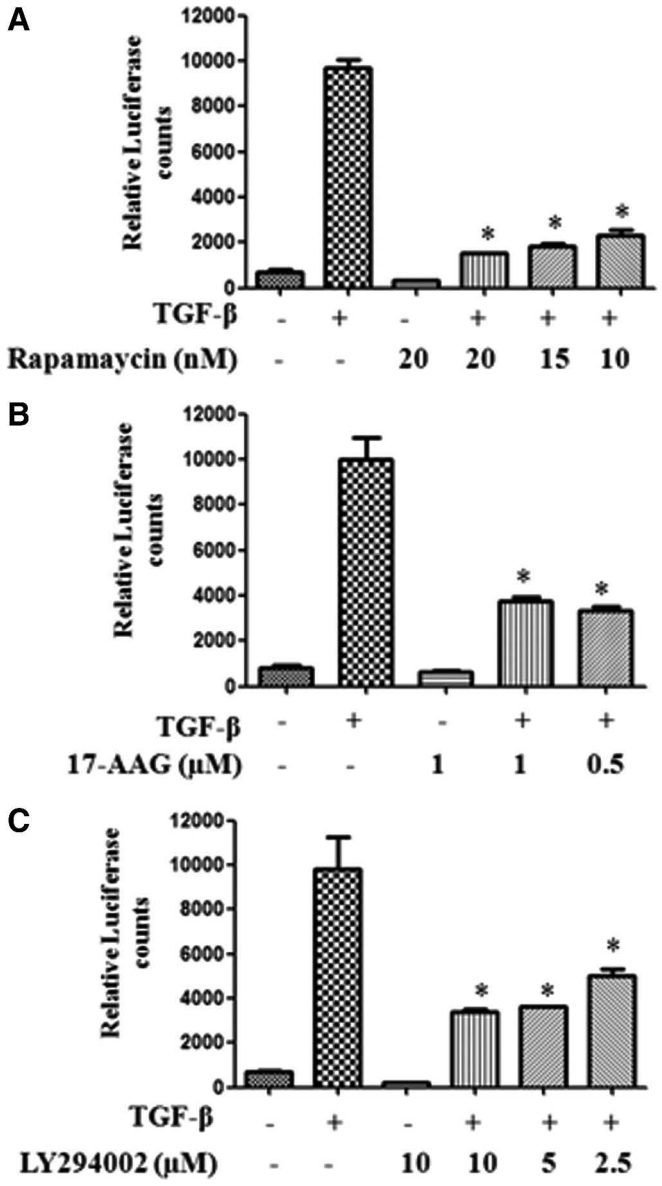

FIGURE 4. Effect of rapamycin, 17-AAG and LY 294002 on transforming growth factor-β (TGF-β)-induced Smad functional activity: A549-SBE-Luc cells were serum starved for 24 hours, stimulated with TGF-β (5 ng/ml) in the presence or absence of inhibitors at indicated concentrations. After 4 hours, luciferase expression was measured and normalized to the protein concentrations. Error bars represent the standard deviation (SD) from three independent replicates. *Statistically significant ($p < 0.05$) difference when compared with TGF-β treated cells.

it is, then how rapamycin is modulating TGF-β signaling. In contrast to rapamycin and 17-AAG, LY294002 had no effect on Smad phosphorylation. Interestingly, LY294002 did significantly inhibit TGF-β-induced Smad transcriptional activity, suggesting a role for the PI3K pathway in the transcriptional regulation of TGF-β signaling.

Earlier reports showed cross-talk between PI3K and mTOR pathways where inhibition of one pathway modulates the other, depending on the cell type and the context. Hence, it was expected that inhibition of PI3K or mTOR may result in similar effects. On the contrary, we observed that rapamycin attenuated both E-cadherin loss and N-cadherin gain, whereas LY294002 selectively inhibited EMT-induced N-cadherin and vimentin expression without affecting the loss of E-cadherin. This suggests that both these compounds have effects that are independent of the cross-talk between them, such as modulation of TGF-β signaling by rapamycin. However, both compounds equally blocked EMT-induced migration, invasion and MMP secretion that strongly suggests a role for both cross-talk dependent and independent pathways.

In addition to these three compounds, we also assessed the effect of acetylsalicyclic acid and novobiocin on TGF-β-induced EMT. At the concentrations tested, both these compounds showed no significant effects on either biochemical or functional markers (migration and invasion) of EMT (data not shown). Apart from migratory and invasive phenotype, EMT is known to confer other functional phenotypes to cancer cells, including growth inhibition, resistance to apoptosis, evasion of immune surveillance and, in certain cases, stem cell-like properties.[2,40] Therefore, it is possible that the compounds that showed no effect on the markers we tested may still affect the other functional phenotypes described earlier to justify their identification as potential EMT inhibitors.

In summary, despite the prevalent notion that rapamycin either potentiates TGF-β signaling[50] or has no effect on EMT,[49] we identified rapamycin as a candidate inhibitor of TGF-β signaling and EMT. Also, in contrast to previous reports,[53] we identified LY294002 as a selective inhibitor of mesenchymal phenotype during EMT. In addition, 17-AAG was identified as a potent EMT inhibitor which was consistent with the role of HSP90 in the stability of TGF-β receptors.[43] Collectively, these results demonstrate the need for such system-wide approaches[54] to look beyond the bias of previous information for gaining new insights.

ACKNOWLEDGMENTS

Supported by NIH/NCI (CA132571-01) and American Cancer Society (RSG-CSM-116801) grants (V.G.K) and Proteomics Alliance for Cancer Research grants from the Michigan Technology Tri-Corridor (MEDC-GR238, MTTC-GR687) (G.S.O.).

REFERENCES

1. Friedl P, Wolf K. Tumour-cell invasion and migration: diversity and escape mechanisms. *Nat Rev Cancer* 2003;3:362–374.
2. Kalluri R, Weinberg RA. The basics of epithelial-mesenchymal transition. *J Clin Invest* 2009;119:1420–1428.
3. Bierie B, Moses HL. Tumour microenvironment: TGFbeta: the molecular Jekyll and Hyde of cancer. *Nat Rev Cancer* 2006;6:506–520.
4. Kasai H, Allen JT, Mason RM, et al. TGF-beta1 induces human alveolar epithelial to mesenchymal cell transition (EMT). *Respir Res* 2005;6:56.
5. Muraoka RS, Dumont N, Ritter CA, et al. Blockade of TGF-beta inhibits mammary tumor cell viability, migration, and metastases. *J Clin Invest* 2002;109:1551–1559.
6. Davies M, Robinson M, Smith E, et al. Induction of an epithelial to mesenchymal transition in human immortal and malignant keratinocytes by TGF-beta1 involves MAPK, Smad and AP-1 signalling pathways. *J Cell Biochem* 2005;95:918–931.

7. Grunert S, Jechlinger M, Beug H. Diverse cellular and molecular mechanisms contribute to epithelial plasticity and metastasis. *Nat Rev Mol Cell Biol* 2003;4:657–665.
8. Thiery JP, Sleeman JP. Complex networks orchestrate epithelial-mesenchymal transitions. *Nat Rev Mol Cell Biol* 2006;7:131–142.
9. Lee JM, Dedhar S, Kalluri R, et al. The epithelial-mesenchymal transition: new insights in signaling, development, and disease. *J Cell Biol* 2006;172:973–981.
10. Gerhold DL, Jensen RV, Gullans SR. Better therapeutics through microarrays. *Nat Genet* 2002;32(Suppl):547–551.
11. Lamb J. The Connectivity Map: a new tool for biomedical research. *Nat Rev Cancer* 2007;7:54–60.
12. Sartor MA, Mahavisno V, Keshamouni VG, et al. ConceptGen: a gene set enrichment and gene set relation mapping tool. *Bioinformatics* 2010;26:456–463.
13. Lamb J, Crawford ED, Peck D, et al. The Connectivity Map: using gene-expression signatures to connect small molecules, genes, and disease. *Science* 2006;313:1929–1935.
14. Zhang SD, Gant TW. A simple and robust method for connecting small-molecule drugs using gene-expression signatures. *BMC Bioinformatics* 2008;9:258.
15. Reka AK, Kurapati H, Narala VR, et al. Peroxisome proliferator activated receptor-γ activation inhibits tumor metastasis by antagonizing Smad3 mediated epithelial mesenchymal transition. *Mol Cancer Ther* 2010;9:3221–3232.
16. Massague J. How cells read TGF-beta signals. *Nat Rev Mol Cell Biol* 2000;1:169–178.
17. Rodina A, Vilenchik M, Moulick K, et al. Selective compounds define Hsp90 as a major inhibitor of apoptosis in small-cell lung cancer. *Nat Chem Biol* 2007;3:498–507.
18. Maloney A, Workman P. HSP90 as a new therapeutic target for cancer therapy: the story unfolds. *Expert Opin Biol Ther* 2002;2:3–24.
19. Papadimitrakopoulou V, Adjei AA. The Akt/mTOR and mitogen-activated protein kinase pathways in lung cancer therapy. *J Thorac Oncol* 2006;1:749–751.
20. Workman P, Clarke PA, Raynaud FI, et al. Drugging the PI3 kinome: from chemical tools to drugs in the clinic. *Cancer Res* 2010;70:2146–2157.
21. Gridelli C, Maione P, Rossi A. The potential role of mTOR inhibitors in non-small cell lung cancer. *Oncologist* 2008;13:139–147.
22. Donnelly A, Blagg BS. Novobiocin and additional inhibitors of the Hsp90 C-terminal nucleotide-binding pocket. *Curr Med Chem* 2008;15:2702–2717.
23. Burlison JA, Neckers L, Smith AB, et al. Novobiocin: redesigning a DNA gyrase inhibitor for selective inhibition of hsp90. *J Am Chem Soc* 2006;128:15529–15536.
24. Chen Q. Nordihydroguaiaretic acid analogues: their chemical synthesis and biological activities. *Curr Top Med Chem* 2009;9:1636–1659.
25. Krysan K, Reckamp KL, Sharma S, et al. The potential and rationale for COX-2 inhibitors in lung cancer. *Anticancer Agents Med Chem* 2006;6:209–220.
26. Swannie HC, Kaye SB. Protein kinase C inhibitors. *Curr Oncol Rep* 2002;4:37–46.
27. Lee MS, Johansen L, Zhang Y, et al. The novel combination of chlorpromazine and pentamidine exerts synergistic antiproliferative effects through dual mitotic action. *Cancer Res* 2007;67:11359–11367.
28. Williams CS, Sheng H, Brockman JA, et al. A cyclooxygenase-2 inhibitor (SC-58125) blocks growth of established human colon cancer xenografts. *Neoplasia* 2001;3:428–436.
29. Winters ME, Mehta AI, Petricoin EF III, et al. Supra-additive growth inhibition by a celecoxib analogue and carboxyamido-triazole is primarily mediated through apoptosis. *Cancer Res* 2005;65:3853–3860.
30. Fontaine E, McShane J, Page R, et al. Aspirin and non-small cell lung cancer resections: effect on long-term survival. *Eur J Cardiothorac Surg* 2010;38:21–26.
31. Liu Y, Zhang Y, Min J, et al. Calcineurin promotes proliferation, migration, and invasion of small cell lung cancer. *Tumour Biol* 2010;31:199–207.
32. Eckstein LA, Van Quill KR, Bui SK, et al. Cyclosporin A inhibits calcineurin/nuclear factor of activated T-cells signaling and induces apoptosis in retinoblastoma cells. *Invest Ophthalmol Vis Sci* 2005;46:782–790.
33. Zhu F, Zhang Z, Wu G, et al. Rho kinase inhibitor fasudil suppresses migration and invasion though down-regulating the expression of VEGF in lung cancer cell line A549. *Med Oncol*.
34. Stork LC, Matloub Y, Broxson E, et al. Oral 6-mercaptopurine versus oral 6-thioguanine and veno-occlusive disease in children with standard-risk acute lymphoblastic leukemia: report of the Children's Oncology Group CCG-1952 clinical trial. *Blood* 2010;115:2740–2748.
35. Quann EJ, Khwaja F, Zavitz KH, et al. The aryl propionic acid R-flurbiprofen selectively induces p75NTR-dependent decreased survival of prostate tumor cells. *Cancer Res* 2007;67:3254–3262.
36. Dinney CP, Parker C, Dong Z, et al. Therapy of human transitional cell carcinoma of the bladder by oral administration of the epidermal growth factor receptor protein tyrosine kinase inhibitor 4,5-dianilinophthalimide. *Clin Cancer Res* 1997;3:161–168.
37. Haince JF, Rouleau M, Hendzel MJ, et al. Targeting poly(ADP-ribosyl)ation: a promising approach in cancer therapy. *Trends Mol Med* 2005;11:456–463.
38. Moon D-O, Kim M-O, Choi YH, et al. Butein sensitizes human hepatoma cells to TRAIL-induced apoptosis via extracellular signal-regulated kinase/Sp1-dependent DR5 upregulation and NF-kappaB inactivation. *Mol Cancer Ther* 2010;9:1583–1595.
39. Shin SY, Choi BH, Ko J, et al. Clozapine, a neuroleptic agent, inhibits Akt by counteracting Ca2+/calmodulin in PTEN-negative U-87MG human glioblastoma cells. *Cell Signal* 2006;18:1876–1886.
40. Thiery JP. Epithelial-mesenchymal transitions in tumour progression. *Nat Rev Cancer* 2002;2:442–454.
41. Roberts AB, Tian F, Byfield SD, et al. Smad3 is key to TGF-beta-mediated epithelial-to-mesenchymal transition, fibrosis, tumor suppression and metastasis. *Cytokine Growth Factor Rev* 2006;17:19–27.
42. Reka AK, Kurapati H, Narala VR, et al. Peroxisome proliferator-activated receptor-gamma activation inhibits tumor metastasis by antagonizing Smad3-mediated epithelial-mesenchymal transition. *Mol Cancer Ther* 2010;9:3221–3232.
43. Wrighton KH, Lin X, Feng XH. Critical regulation of TGFbeta signaling by Hsp90. *Proc Natl Acad Sci USA* 2008;105:9244–9249.
44. Vilar E, Mukherjee B, Kuick R, et al. Gene expression patterns in mismatch repair-deficient colorectal cancers highlight the potential therapeutic role of inhibitors of the phosphatidylinositol 3-kinase-AKT-mammalian target of rapamycin pathway. *Clin Cancer Res* 2009;15:2829–2839.
45. De Preter K, De Brouwer S, Van Maerken T, et al. Meta-mining of neuroblastoma and neuroblast gene expression profiles reveals candidate therapeutic compounds. *Clin Cancer Res* 2009;15:3690–3696.
46. Hassan SB, Gali-Muhtasib H, Goransson H, et al. Alpha terpineol: a potential anticancer agent which acts through suppressing NF-kappaB signalling. *Anticancer Res* 2010;30:1911–1919.
47. Wullschleger S, Loewith R, Hall MN. TOR signaling in growth and metabolism. *Cell* 2006;124:471–484.
48. Ebi H, Tomida S, Takeuchi T, et al. Relationship of deregulated signaling converging onto mTOR with prognosis and classification of lung adenocarcinoma shown by two independent in silico analyses. *Cancer Res* 2009;69:4027–4035.
49. Lamouille S, Derynck R. Cell size and invasion in TGF-beta-induced epithelial to mesenchymal transition is regulated by activation of the mTOR pathway. *J Cell Biol* 2007;178:437–451.
50. Chen Y-G, Liu F, Massague J. Mechanism of TGF[beta] receptor inhibition by FKBP12. *EMBO J* 1997;16:3866–3876.
51. Huse M, Muir TW, Xu L, et al. The TGF beta receptor activation process: an inhibitor- to substrate-binding switch. *Mol Cell* 2001;8:671–682.
52. Wang T, Donahoe PK, Zervos AS. Specific interaction of type I receptors of the TGF-beta family with the immunophilin FKBP-12. *Science* 1994;265:674–676.
53. Bakin AV, Tomlinson AK, Bhowmick NA, et al. Phosphatidylinositol 3-kinase function is required for transforming growth factor beta-mediated epithelial to mesenchymal transition and cell migration. *J Biol Chem* 2000;275:36803–36810.
54. Woolf PJ, Alvarez A, Keshamouni VG. Systems approach for understanding metastasis. In Keshamouni VG, Arenberg DA, Kalemkerian GP (Eds). Lung Cancer Metastasis: Novel Biological Mechanisms and Impact on clinical Practice. New York, NY: Springer, 2009. Pp. 383–394.